Forecasting September Atlantic Basin Tropical Cyclone Activity

PHILIP J. KLOTZBACH AND WILLIAM M. GRAY

Department of Atmospheric Science, Colorado State University, Fort Collins, Colorado

(Manuscript received 12 November 2002, in final form 24 June 2003)

ABSTRACT

September is the most active month for Atlantic basin tropical cyclone activity with about 50% of all hurricane activity occurring during this month. Utilizing National Centers for Environmental Prediction–National Center for Atmospheric Research (NCEP–NCAR) reanalysis data, a prediction scheme for forecasting September tropical cyclone activity has been developed. Based on hindcasting results from 1950 to 2000, 30%–75% of the variance for most tropical cyclone parameters can be hindcast by the end of July. This hindcast skill improves to 45%–75% by the end of August. Similarly, cross-validated hindcast skill explains from 20% to 65% for most variables by the end of July, improving to 30%–65% by the end of August. Simple least squared linear regression was utilized to calculate hindcast skill, and variables were selected that explained the largest degree of variance when combined with the other predictors in the scheme. These predictors tend to be global in nature and include zonal and meridional wind at 200 and 1000 mb and sea level pressure measurements at various global locations. Many of the predictors are strongly correlated with global modes such as El Niño–Southern Oscillation (ENSO) or the Pacific decadal oscillation (PDO). Based on this September hurricane prediction scheme, U.S. tropical cyclone landfall probability forecasts can also be issued. In addition, the 1 August forecast of September activity can also be applied to improve the hindcast skill of Gray's 1 August seasonal statistical forecast.

1. Introduction

Although Atlantic basin seasonal hurricane forecasting has undergone much study and predictions have been made over the past 20 yr (Gray 1984), the development of short-term forecasts on monthly and submonthly timescales has until recently not been attempted. Intraseasonal hurricane prediction is useful because many active seasons have inactive periods and vice versa. For example, though 1995 was the most active tropical cyclone season since 1950, only 2 of the 11 hurricanes that year formed during the climatologically most active month of September. During 1997, an inactive year, four named storms formed during July while only one hurricane formed after 1 August, which, climatologically, accounts for over 90% of the season. Many other examples of active and inactive periods during a hurricane season can be drawn from the data. These short-term forecasts also offer the prospect for obtaining a better understanding of how the atmosphere functions.

Ballenzweig (1959) was one of the first researchers to consider monthly large-scale atmospheric circulation trends associated with variations in Atlantic hurricane frequency. He composited five active and five inactive August–October periods and evaluated the prevailing 700-mb geopotential height field during those years. Deeper easterlies were prevalent during active seasons, and the Atlantic subtropical high was displaced farther northward. He argued that this information would be useful in forecasting shorter (i.e., monthly) timescales.

Shapiro (1987) delved into monthly hurricane prediction by utilizing EOF analysis and found that a Walker cell circulation associated with ENSO was the first EOF in zonal wind variability at lower and upper levels in the tropical Atlantic. (See the appendix for a list of the key symbols and acronyms used in this paper.) El Niño conditions were associated with more anticyclonic vorticity at low levels and increased vertical shear in the prime tropical cyclone development region in the Atlantic. He found that predictive skill explaining about 45% of the variance of a particular month's tropical cyclone activity could be obtained 1–2 months in advance. Shapiro found that an El Niño index explained only 7% of the variance. This implied that a large amount of the explained variance was due to global circulation features not directly related to ENSO.

More recently, Maloney and Hartmann (2000) found that there were dramatic differences in tropical cyclone formation in the Gulf of Mexico and Caribbean Sea, which were associated with different phases of the Madden–Julian oscillation (MJO). They stated that hurricane formation in the western Caribbean Sea and the Gulf of Mexico was 4 times more likely during the active (west)

Corresponding author address: Philip J. Klotzbach, Dept. of Atmospheric Science, Colorado State University, Fort Collins, CO 80523.
E-mail: philk@atmos.colostate.edu

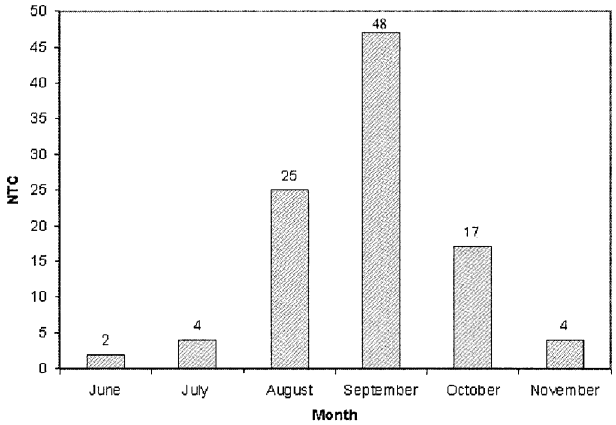

FIG. 1. NTC activity in the Atlantic basin by month (1950–2000).

TABLE 1. Sep climatological (1950–2000) values of named storms, named storm days, hurricanes, hurricane days, intense hurricanes, intense hurricane days, and NTC activity. Total year averages are shown in parentheses. NTC for Sep is calculated by taking 100 times one-sixth of the sum of the following ratios: 3.4/9.6 = 35, 21.7/49.1 = 44, 2.4/5.9 = 41, 12.3/24.5 = 50, 1.3/2.3 = 57, and 3.0/5.0 = 60 for an NTC of 48.

Parameter	Sep climatological values (1950–2000)
Named storms (NS) (9.6)	3.4
Named storm days (NSD) (49.1)	21.7
Hurricanes (H) (5.9)	2.4
Hurricane days (HD) (24.5)	12.3
Intense hurricanes (IH) (2.3)	1.3
Intense hurricane days (IHD) (5.0)	3.0
Net tropical cyclone activity (NTC) (100)	48.0

phase of the MJO than during the inactive (east) phase. Their MJO index was created by averaging 850-mb winds over the eastern Pacific Ocean, and winds that were greater than one standard deviation from the west were classified as west phase. Conversely winds that were greater than one standard deviation from the east were classified as east phase. Active phases of the MJO were associated with cyclonic vorticity in the Caribbean Sea and the Gulf of Mexico providing favorable conditions for development; whereas, anticyclonic vorticity anomalies were prevalent during the east phase.

Blake (2002) has recently begun issuing forecasts of August tropical cyclone (TC) activity with considerable success through utilizing reanalysis data from the National Centers for Environmental Prediction (NCEP) and the National Center for Atmospheric Research (NCAR) (Kalnay et al. 1996). Reanalysis datasets provide daily and monthly data world wide for a plethora of variables such as zonal wind and geopotential height at a variety of levels. Blake found that, using a 12-predictor model, 50%–80% of the variance in August Atlantic basin tropical cyclone activity could be hindcast by 1 August based on 51 yr of data (1949–99).

Since September is climatologically the most active month of the Atlantic hurricane season, it is to the forecasting of September Atlantic basin tropical cyclones that we now turn our attention. A look at September climatology from 1950 to the present is the subject of section 2, and section 3 investigates the methodology adopted for developing the forecast scheme. Section 4 applies the predictors obtained from 51 yr (1950–2000) of hindcast data. Physical explanations as to why the predictors selected alter hurricane activity will be discussed in section 5. Objective statistical significance tests will be applied to the predictors in section 6, and two applications of the forecast scheme are discussed in section 7. Conclusions and future work are the topics of section 8.

2. September climatology

September is the most prolific month for tropical cyclone activity in the Atlantic basin. According to the National Hurricane Center's Atlantic track files, September accounted for 48% of all tropical cyclone activity between 1950 and 2000 with August and October accounting for most of the remainder. Figure 1 gives a graphical illustration of tropical cyclone activity by month. Monthly tropical cyclone activity is depicted as net tropical cyclone (NTC) activity, which is an aggregate measure of the following six parameters: named storms (NS), named storm days (NSD), hurricanes (H), hurricane days (HD), intense hurricanes (IH), and intense hurricane days (IHD). See the appendix for complete definitions of the six parameters used to calculate NTC. NTC is a weighted average of these six parameters relative to their climatological value, and therefore average annual NTC is 100. By definition, a year with above-average tropical cyclone activity will have an NTC value greater than 100.

Climatological average activity for September and an example NTC calculation are listed in Table 1. Placing the average September values of each parameter in the NTC calculation yields a mean value for September NTC of 48 for the period 1950–2000. Tropical cyclone activity during September has ranged considerably during 1950–2002, from one to eight named storms, zero to five hurricanes, and zero to four intense hurricanes. Storms were counted as September storms if they reached named storm ($\geq$34 kt), hurricane ($\geq$64 kt), or intense hurricane ($\geq$96 kt) status for the first time between 0000 UTC 1 September and 1800 UTC 30 September. If a storm was already a named storm on 29 August and became a hurricane on 2 September, it would count as zero named storms and one hurricane, thereby explaining how it is possible that one year can have more hurricanes then named storms. In addition, intense tropical cyclones before 1970 were required to have reached an intensity of 105 kt (versus 100 kt after 1970)

due to the overestimation bias problem during the earlier decades as discussed in Landsea (1993). Although surface pressure measurements have not changed much since the 1950s, observational measurements of winds have improved considerably since 1970. Observed winds of intense hurricanes in the National Hurricane Center's ''best track'' dataset for a given pressure have decreased by about 5 kt since 1970, and since wind measurements have improved, it is assumed that wind intensities of intense hurricanes prior to 1970 were overestimated. Therefore tropical cyclones prior to 1970 are required to have reached 105 kt to be classified as an intense hurricane. Table 2 displays the September tropical cyclone statistics from 1950 to 2002.

The ''TO'' in the last two columns of Table 2 refers to tropical-only named storms (TONS) and tropical-only hurricanes (TOH), which basically denotes storms originating from Africa-spawned easterly waves equatorward of 25°N. Storms were classified as TONS if they developed from easterly waves into tropical storms with no aid from baroclinic influences such as upper-level troughs or frontal boundaries. If a TONS developed into a hurricane with no assistance from the middle latitudes, it was classified as a TOH. If an easterly wave developed into a named storm with no midlatitude assistance but was aided by a frontal boundary in its intensification into a hurricane, it would be classified as a TONS but not a TOH. More complete definitions of tropical-only named storms and tropical-only hurricanes are discussed in Blake (2002) for TONS and Elsner et al. (1996) for TOH. September's ratio of tropical-only/baroclinic systems is larger than any other month of the Atlantic tropical cyclone season; that is, the odds are greater that a particular storm in September will have its genesis from an Africa-spawned easterly wave than in another month of the hurricane season.

Cross correlations between September tropical cyclone parameters range from as low as 0.19 between named storms and intense hurricane days to as high as 0.92 between named storm days and hurricane days. Since some of these parameters only correlate weakly with each other, it is not surprising that distinct sets of global predictors are selected to forecast the various TC parameters.

Landfalling tropical cyclones are a fairly common occurrence during the month of September. Between 1950 and 2000, 51 named storms made landfall along the United States coast, of which 16 were category 1–2 hurricanes on the Saffir–Simpson scale (Simpson 1974), and 16 were intense (categories 3–5) hurricanes. The most recent intense September landfalling hurricane of note was Hugo in 1989, which caused 21 deaths in the United States and cost more than $7 billion in damage according to the National Hurricane Center's preliminary report. Climatologically, the probability of a U.S. landfall during any given September is 67% for named storms, 49% for hurricanes, and 29% for intense hurricanes. Intense hurricane landfalls are much more likely during active Septembers than inactive Septembers. During the 15 least active Septembers between 1950 and 2000, there were no intense hurricane landfalls. Conversely, the 15 most active Septembers had seven intense hurricane landfalls. Intense hurricane landfalls are especially devastating, because, according to Pielke and Landsea (1998), intense hurricanes cause about 85% of all tropical cyclone–related damage even though they make up only one-quarter of all named storms. Accurately forecasting September tropical cyclone activity can translate into useful information regarding the likelihood of a tropical cyclone striking the U.S. coast. An accurate landfall probability forecast provides valuable advanced notice to emergency planners and coastal residents alike about the likelihood of a hurricane making landfall during a particular year.

3. Methodology

The objective of the September Atlantic basin tropical cyclone forecast was to find the predictive parameters that maximized the hindcast skill during the period 1950–2000. Hindcasting involved selecting reasonable predictors that explained the most variance in tropical cyclone activity during the period being hindcast. The predictor selection process began by constructing top 10–bottom 10 composite maps of various meteorological parameters such as sea surface temperature, sea level pressure, and zonal wind at 200, 850, and 1000 mb for the month of September by differencing active and inactive Septembers. Activity for a particular September was based on the NTC activity parameter, and difference maps were constructed utilizing the Climate Diagnostics Center's (CDC) Monthly/Seasonal Climate Composites Web page (http://www.cdc.noaa.gov/cgi-bin/Composites/printpage.pl). That is, composite difference maps were constructed for the reanalysis fields based upon the top 10 highest NTC Septembers minus the bottom 10 lowest NTC Septembers. Difference maps between active and inactive Septembers showed the features that were prevalent during most active Septembers but absent during most inactive Septembers or vice versa. Many of the global tropical cyclone activity linked features clearly appeared on these maps, including low sea level pressure in the tropical Atlantic, La Niña conditions in the Pacific, and easterly zonal wind anomalies at 200 mb throughout most of the Tropics for active Septembers. This result adds confidence to the NCEP–NCAR reanalysis calculations since they agree qualitatively with previous detailed case study research by Ballenzweig, Gray, Shapiro, Elsner, and others.

After examination of the lag-0 composite maps for September, composites of meteorological parameters during the preceding Augusts were generated to see what kind of predictive signals might exist for September activity. Many of the same atmospheric features that appeared in active Septembers also occurred during Augusts prior to

TABLE 2. Climatological summary of Sep tropical cyclone activity from 1950 to 2002. The largest values for any tropical cyclone parameter are shown in boldface, and the smallest values are in italics. The acronyms of the head of each column are defined in the appendix.

Year	NS	NSD	H	HD	IH	IHD	NTC	TONS	TOH
1950	3	34.25	2	25.75	3	10.75	97.6	2	2
1951	3	23.00	3	17.00	1	3.25	51.1	3	3
1952	2	19.00	3	12.75	2	3.00	51.6	2	3
1953	4	26.25	4	14.00	3	5.75	77.6	3	4
1954	4	15.25	3	7.25	1	2.50	41.1	3	3
1955	5	37.50	**5**	25.75	3	5.75	94.0	**5**	**5**
1956	4	13.00	1	1.50	*0*	*0.00*	15.2	3	1
1957	4	28.00	2	18.75	1	4.75	57.9	2	1
1958	4	27.25	3	13.00	2	3.00	58.0	4	3
1959	3	13.75	3	10.50	1	1.00	36.1	1	1
1960	2	16.25	2	12.75	2	9.00	67.8	1	1
1961	6	**44.50**	4	**34.00**	**4**	**15.75**	**141.4**	**5**	4
1962	*1*	3.75	*0*	*0.00*	*0*	*0.00*	*3.0*	1	*0*
1963	5	15.25	4	7.00	1	0.25	38.0	3	3
1964	5	44.00	4	30.50	2	3.75	82.7	**5**	4
1965	2	24.75	1	20.00	1	6.50	57.2	2	1
1966	4	16.00	1	10.00	1	2.75	38.4	3	1
1967	4	41.50	4	28.25	1	5.75	78.0	3	2
1968	2	6.00	*0*	*0.00*	*0*	*0.00*	5.5	1	*0*
1969	5	20.25	**5**	9.00	1	0.50	44.7	2	3
1970	3	5.50	1	2.00	1	0.50	20.2	2	*0*
1971	6	43.50	4	25.50	1	0.75	63.6	3	2
1972	*1*	10.25	1	1.25	*0*	*0.00*	8.9	*0*	*0*
1973	2	13.75	1	3.75	1	0.25	21.6	1	*0*
1974	4	22.50	2	10.50	1	2.75	43.8	3	2
1975	3	25.75	3	13.75	1	0.50	40.7	3	3
1976	*1*	10.50	1	8.75	1	0.25	22.2	*0*	*0*
1977	3	9.25	3	4.50	1	1.00	30.5	*0*	*0*
1978	3	25.50	2	10.75	2	3.50	53.0	1	1
1979	2	30.00	3	16.00	1	1.75	46.1	*0*	1
1980	5	27.25	3	15.50	1	0.75	46.7	3	2
1981	5	39.25	**5**	20.75	3	3.75	84.5	4	4
1982	2	9.50	1	5.25	1	1.25	24.5	*0*	*0*
1983	2	7.00	1	1.25	*0*	*0.00*	9.5	*0*	*0*
1984	6	26.00	2	3.75	1	0.75	37.2	1	*0*
1985	3	16.25	1	8.00	2	3.00	43.5	1	1
1986	2	10.00	1	7.25	*0*	*0.00*	14.6	1	*0*
1987	3	16.75	1	2.75	1	0.50	24.5	3	1
1988	7	26.50	4	16.25	2	6.75	80.5	**5**	3
1989	2	32.25	3	20.00	2	9.75	83.5	2	2
1990	2	16.00	1	10.00	*0*	*0.00*	18.5	1	1
1991	3	11.75	1	3.75	1	1.00	25.2	2	*0*
1992	4	22.50	2	9.50	*0*	*0.00*	26.7	*0*	*0*
1993	3	12.00	3	5.00	*0*	0.50	22.8	1	1
1994	2	*3.25*	*0*	*0.00*	*0*	*0.00*	4.6	2	*0*
1995	3	28.25	2	22.50	2	8.75	79.4	3	2
1996	2	23.00	2	17.50	3	5.00	67.2	2	2
1997	*1*	12.25	1	7.25	1	2.25	28.4	1	1
1998	6	42.75	**5**	28.00	1	2.25	72.8	2	2
1999	3	27.00	2	15.75	2	9.25	76.1	3	2
2000	7	29.50	**5**	13.50	1	2.75	61.9	**5**	3
2001	4	29.25	4	15.50	2	2.00	59.9	1	1
2002	**8**	35.50	4	7.75	1	1.50	54.8	2	2
Mean	3.5	22.07	2.4	12.29	1.3	2.96	47.8	2.1	1.6
Median	3.0	22.50	2.0	10.50	1.0	2.00	44.7	2.0	1.0
Std dev	1.7	11.28	1.4	8.64	0.9	3.41	28.4	1.4	1.4

the active Septembers including easterly anomalies at 200 mb and low sea level pressure in the tropical Atlantic. Most sea surface temperature patterns persisted from August through September including warm sea surface temperatures in the Atlantic and cool temperatures in the tropical eastern Pacific. One advantage to features that persist from month to month during active seasons is that the physics linking these features to variable TC activity are fairly well explained in previous studies thus adding confidence to their inclusion in a forecast scheme. Climate signals several months in advance were also examined in accordance with the findings of Shapiro (1987).

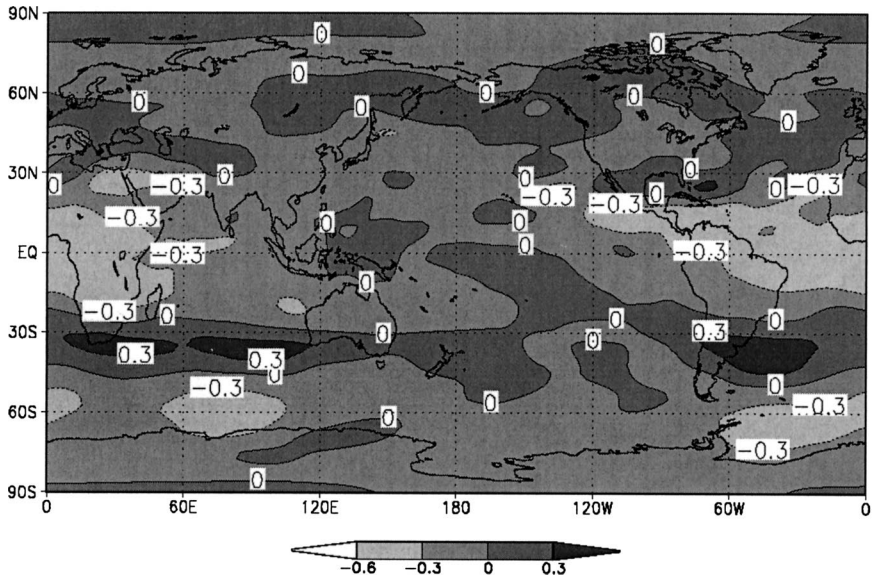

FIG. 2. Correlation map between Sep NTC and Aug 200-mb zonal wind. Note that the large area in the Tropics shaded in light gray correlated at ($r < -0.3$).

Another tool used in the selection of predictors was the Climate Diagnostic Center's Linear Correlations Web page (http://www.cdc.noaa.gov/Correlation), which allowed for testing correlations between global data fields and TC activity time series created by the user, such as September hurricane days or NTC. Correlations between September tropical cyclone activity and September global atmospheric data fields were plotted first, and then correlation maps between earlier months and September activity were constructed. Figures 2 and 3 show the correlation between September NTC and August 200-mb zonal wind and the correlation between September NTC and September 200-mb zonal wind, respectively. Note the similar locations of strong correlations when August conditions are used to forecast September activity. Hence, part of forecasting September tropical cyclone activity consists of knowing that certain basic oceanic and atmospheric features in August are likely to persist through September. However, simply utilizing persistence of large-scale atmospheric and oceanic features to forecast tropical cyclones still leaves large amounts of unexplained variance.

One final approach used to select predictors for the September forecast was utilizing a residual. For this,

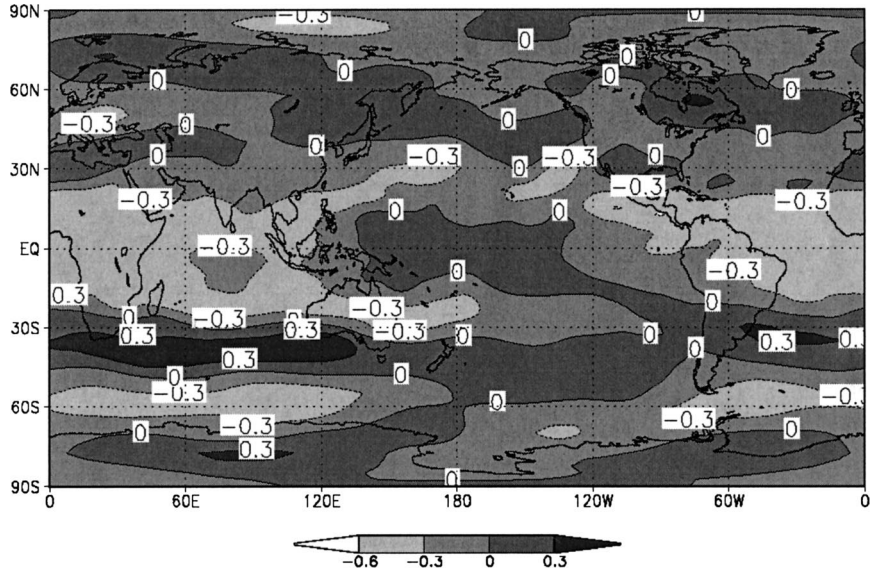

FIG. 3. Correlation map between Sep NTC and Sep 200-mb zonal wind. Note that the large area in the Tropics shaded in light gray correlated at ($r < -0.3$).

TABLE 3. Predictors selected for the 1 Aug forecast. The sign of the predictor associated with increased tropical cyclone activity based on the simple correlation with the predictand is in parentheses. Note that predictors 6 and 7 are not used since they require Aug data.

Predictor	Location	Equations used
1) Apr S Atlantic 1000-mb U (−)	12.5°–30°S, 40°W–10°E	IH
2) Jul Asian 200-mb geopotential height (+)	32°–42°N, 100°–160°E	NS, NSD, H, HD, IH, TONS, TOH, NTC
3A) Jul Atlantic 1000-mb U (+)	5°–15°N, 30°–50°W	NS, NSD, H, HD, IH, IHD, TONS, TOH, NTC
4) Feb W African 1000-mb U (−)	20°–30°N, 15°W–15°E	NSD, HD, IHD, NTC
5) April NE Siberian 200-mb U (−)	67.5°–85°N, 110°E–180°	NS, NSD, HD, IH, IHD, TONS, TOH, NTC
8) May central African 200-mb V (+)	0°–20°S, 15°–30°E	NSD, H, HD
9) Jan–Feb W Pacific 200-mb U (−)	15°–25°N, 120°E–160°W	IH, IHD, TONS, TOH, NTC

one or two predictors already in the forecast model were used to predict the TC variable in question, for example, NTC. The difference between actual value minus forecast value for each year was considered a residual, and a time series of these residuals was created. Correlation maps between these residual time series and global atmospheric and oceanic features were then constructed to see if there were any large-scale areas that correlated strongly with both the residual and the predictand itself. A primary predictor selected utilizing this technique was the May 200-mb meridional wind component V over central Africa. Partial correlations, that is, the correlation associated with a particular predictor given the other predictors already in the model, were calculated to determine if a significant improvement to the forecast equation could be made with the addition of the new predictor (Neter et al. 1983). All predictors added to the model had partial correlations greater than a value of 0.25, which is significant at greater than the 90% significance level. For reference, partial correlations of 0.27 and 0.34 are significant at the 95% and 99% level, respectively, using a two-tailed Student's t test. It should also be noted that all areas in the forecast model had to be of relatively large spatial extent so that large-scale atmospheric patterns were being considered. Such large area extents eliminate selection of local ''bull's-eye'' features that are prevalent on some of the correlation maps. No parameter was added to the forecast model that spanned an area less than 10° by 20°.

4. Results

An initial attempt at forecasting September tropical cyclone activity was done by simply utilizing values of well-known global modes (i.e., ENSO, PDO, NAO, AO, etc.). Very little hindcast skill was achieved using this technique since many of these global modes are quite strongly related (i.e., ENSO and the PDO, the NAO and AO), and modes such as the North Atlantic Oscillation are ill-defined over the summer months. We then turned our attention to regions of the globe that correlated strongly with tropical cyclone activity according to the NCEP–NCAR reanalysis.

There were 126 predictors screened for potential forecast ability, but many of these were rejected because they correlated strongly with other predictors already in the scheme and therefore provided redundant information. Other predictors were removed from the predictor pool because the correlation changed sign or was considerably reduced when the 51-yr time series was subdivided. Approximately 25 predictors were inserted into the model, but there were only 9 predictors that had significant partial correlations with September tropical cyclone activity while also correlating at least moderately ($r \sim 0.3$) with the predictand itself. The final list of predictors selected utilizing the methodology described in the previous section for the 1 August forecast are listed in Table 3. The 1 September forecast predictors are listed in Table 4, and Fig. 4 shows the geographic location of all the predictors. Note that the Atlantic 1000-mb wind predictor utilizes only the tropical component for the 1 August predictor and is denoted as predictor 3A. The September version of this predictor takes the difference between the 1000-mb winds in the tropical Atlantic and the 1000-mb winds in the subtropical Atlantic. The area in the subtropical Atlantic is denoted as predictor 3B, and hence the 1 September version of this predictor is denoted as 3A–3B throughout

TABLE 4. As in Table 3 but for the 1 Sep forecast.

Predictor	Location	Equations used
1) Apr S Atlantic 1000-mb U (−)	12.5°–30°S, 40°W–10°E	IH
2) Jul Asian 200-mb geopotential height (+)	32°–42°N, 100°–160°E	NSD, H, IH, TONS, TOH, NTC
3A–3B) Jul–Aug Atlantic 1000-mb U (+) (−)	5°–15°N, 30°–50°W 22.5°–35°N, 35°–65°W	H, HD, IH, IHD, TONS, TOH, NTC
4) Feb W African 1000-mb U (−)	20°–30°N, 15°W–15°E	NS, NSD, HD, IHD, NTC
5) Apr NE Siberian 200-mb U (−)	67.5°–85°N, 110°E–180°	NS, NSD, HD, IH, IHD, TONS, TOH, NTC
6) Aug Indonesian SLP (−)	0°–30°S, 120°–160°E	NS, NSD, HD, TONS
7) Aug S Indian Ocean SLP (−)	20°–45°S, 60°–90°E	NS, H
8) May central African 200-mb V (+)	0°–20°S, 15°–30°E	NS, NSD, H, HD, IH, TONS, NTC
9) Jan–Feb W Pacific 200-mb U (−)	15°–25°N, 120°E–160°W	IHD, TOH

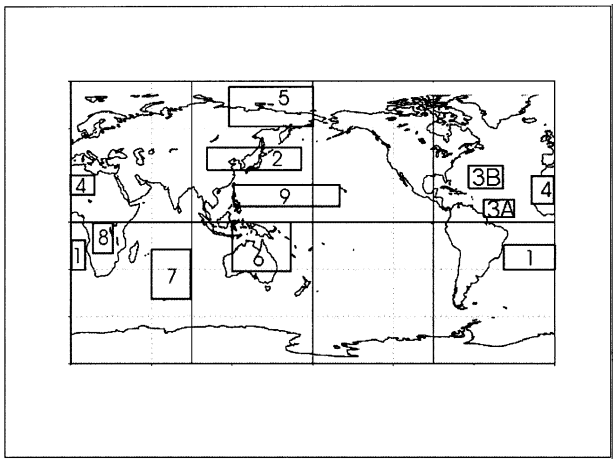

FIG. 4. Location of predictors used in the Sep Atlantic basin tropical cyclone forecast. The numbers in each area are keyed to the description given in Table 4.

the remainder of the text. Tables 5 and 6 display values of hindcast variance explained during 1950–2000 for the 1 August and 1 September predictions of September tropical cyclone activity, respectively. The adjusted variance explained is a modified measure that accounts for the number of predictors in the forecast equation and reduces the hindcast variance explained accordingly.

The reader may note that the hindcast variance explained for NTC did not increase from the 1 August to the 1 September forecast. Shapiro (1987) found a similar result with his initial investigation into forecasting monthly tropical cyclone activity. He found that the correlation between zonal winds in the Atlantic and tropical cyclone activity was just as strong if, for example, July winds were correlated with September tropical cyclone activity compared with a contemporaneous correlation between September zonal winds and September tropical cyclone activity. Two main conclusions were drawn from his research: 1) large-scale features favorable for tropical cyclone activity establish themselves 2 or more months in advance, and 2) some of the weakening of contemporaneous correlations and correlations 1 month in advance may be due to the tropical cyclones themselves. Note also that hindcast skill of weaker storms such as named storms and hurricanes increased considerably from the 1 August hindcast to the 1 September hindcast.

It should be noted that all predictors selected utilize reanalysis ''A'' variables, which according to Kalnay et al. (1996) are primarily observation driven and therefore are mostly reliable. Areas south of 45°S are susceptible to artificial trends in sea level pressure and other reanalysis fields after satellite data began being assimilated in 1979, and therefore all predictors selected are north of 45°S. We have applied a 5-yr running mean to our oceanic predictors and correlated these detrended predictors with net tropical cyclone activity (not shown), and the linear correlation values are only slightly reduced from using the actual yearly observed values of these predictors.

TABLE 5. Variance (r^2) explained, adjusted variance explained, and jackknife variance explained for each of the nine TC activity indices based on the 1 Aug hindcast of Sep tropical cyclone activity from 1950 to 2000.

Parameter	No. of predictors	Variance explained	Adjusted variance explained	Jackknife variance explained
NS	3	0.29	0.24	0.19
NSD	5	0.54	0.49	0.44
H	3	0.38	0.34	0.28
HD	5	0.60	0.56	0.51
IH	5	0.63	0.59	0.53
IHD	4	0.63	0.60	0.54
TONS	4	0.50	0.45	0.40
TOH	4	0.63	0.60	0.55
NTC	5	0.75	0.72	0.68

The jackknife variance explained in Tables 5 and 6 is calculated by computing a forecast value for each year in the 51-yr dataset based on the relationship in the other 50 yr of dependent data. For example, an estimate of 1950 activity would be issued based on equations developed from 1951 to 2000, and this process would be repeated iteratively for 1951, 1952, etc. while changing the test year and dependent dataset accordingly. The resulting values for each year based on the associated independent forecasts are correlated against the predictor time series, and the resulting variance explained provides a more accurate measure of ''real time'' forecasting ability.

Predictors were selected using an all-subset technique. This procedure effectively selects the predictor that explains the most variance for a particular tropical cyclone index, the two predictors that when combined explain the most variance for a particular tropical cyclone index, etc. Additional predictors were added until the variance explained increased less than 3% through the addition of a new predictor to the forecast equation or until five variables were selected. Another method of viewing this stipulation is by considering partial correlations. As mentioned earlier, a partial correlation is

TABLE 6. As in Table 5 but for variance (r^2) explained based on the 1 Sep hindcast of Sep tropical cyclone activity from 1950 to 2000.

Parameter	No. of predictors	Variance explained	Adjusted variance explained	Jackknife variance explained
NS	5	0.45	0.39	0.31
NSD	5	0.63	0.59	0.55
H	4	0.46	0.41	0.36
HD	5	0.67	0.63	0.59
IH	5	0.63	0.59	0.52
IHD	4	0.62	0.58	0.52
TONS	4	0.51	0.46	0.39
TOH	4	0.56	0.52	0.48
NTC	5	0.75	0.73	0.68

TABLE 7. Partial correlations for the addition of individual predictors to the 1 Aug and 1 Sep forecast equations.

1 Aug forecast	First predictor	Second predictor	Third predictor	Fourth predictor	Fifth predictor
NS	0.38	0.31	0.28	—	—
NSD	0.48	0.42	0.35	0.34	0.27
H	0.47	0.38	0.27	—	—
HD	0.49	0.44	0.45	0.36	0.27
IH	0.56	0.47	0.39	0.33	0.31
IHD	0.55	0.53	0.37	0.38	—
TONS	0.54	0.40	0.29	0.27	—
TOH	0.67	0.45	0.29	0.27	—
NTC	0.61	0.47	0.47	0.45	0.41
1 Sep forecast	**First predictor**	**Second predictor**	**Third predictor**	**Fourth predictor**	**Fifth predictor**
NS	0.45	0.30	0.31	0.32	0.26
NSD	0.48	0.42	0.37	0.47	0.37
H	0.50	0.39	0.29	0.26	—
HD	0.58	0.49	0.39	0.37	0.33
IH	0.56	0.46	0.39	0.35	0.37
IHD	0.58	0.51	0.30	0.37	—
TONS	0.50	0.39	0.31	0.28	0.28
TOH	0.61	0.43	0.26	0.27	—
NTC	0.64	0.54	0.45	0.35	0.39

the correlation between a particular predictor with the variable being forecast given the other predictors already in the forecast model. An addition of at least 3% to the variance explained amounted to partial correlations exceeding 0.25, which exceeds the 90% confidence level using a two-tailed Student's *t* test. Partial correlations for the addition of each predictor to the forecast scheme are displayed in Table 7. The restriction to no more than five predictors was intended to minimize statistical overfitting. Total variance explained varied widely from one variable to another, ranging from approximately 30% for named storms hindcast on 1 August to 75% for NTC for both the 1 August and 1 September hindcasts.

Figure 5 shows a graphical depiction of the cross-validated 1 August hindcast of hurricane days compared to what was observed. Figure 6 gives a similar depiction but for the cross-validated 1 September hindcast of NTC compared to what was observed. These two figures were constructed by calculating each year's tropical cyclone activity utilizing a forecast equation developed on the other 50 yr of dependent data. The year being forecast is left out of the developmental equation to better represent the predictive ability of the forecast model. Note that the cross-validated hindcast generally increases and decreases on a year-to-year basis with the degree of hurricane activity. These findings indicate that, assuming that the atmosphere works in the future like it did during the 51-yr hindcast period, there is likely to be some predictive skill with this September tropical cyclone forecast.

Correlations between individual predictors are displayed in Table 8. In general, these individual parameters are little correlated with each other ($r < |0.3|$).

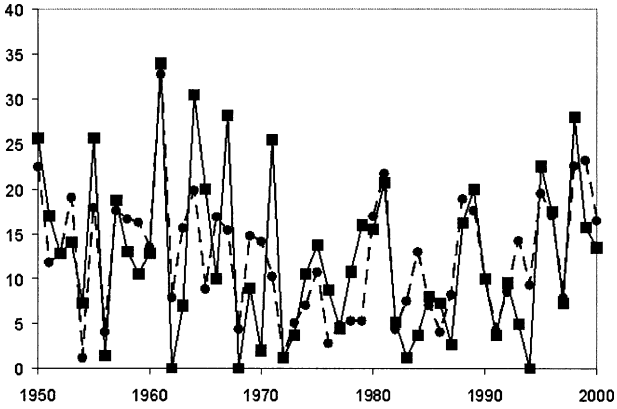

FIG. 5. The 1 Aug cross-validated hindcast (dashed line) of Sep hurricane days vs observations (solid line). Cross-validated (jackknifed) variance (r^2) explained is 0.51.

These minimal correlations between individual predictors imply that each predictor provides considerable independent information. A basic objective in this type of forecast scheme is to select predictors that are uncorrelated with one another so that the maximum amount of new information is obtained with the addition of each new predictor to the forecast.

Table 9 lists correlations between predictors and the September values of various global modes such as ENSO and the PDO. Many of the predictors correlated significantly ($r > |0.3|$) with at least one of the major global modes; however, predictors 4, 8, and 9 correlated little with any of the major indices. These small correlations for the three predictors listed above indicate that atmospheric conditions other than directly linked effects from global modes are likely at work. That is, strong correlations between the predictor and September tropical cyclone activity are likely originating from teleconnected effects not realized in these global modes.

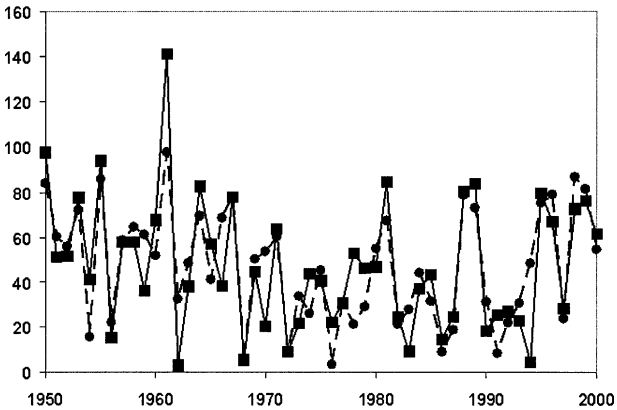

FIG. 6. As in Fig. 5 but for the 1 Sep cross-validated hindcast (dashed line) of Sep NTC vs observations (solid line). Cross-validated (jackknifed) variance (r^2) explained is 0.68.

TABLE 8. Correlations between individual predictors for the 1 Sep forecast. Most intercorrelations are below $r = |0.3|$. Average intercorrelations are computed without respect to sign.

Predictor	1	2	3	4	5	6	7	8	9
1) Apr S Atlantic 1000-mb *U*	—	−0.18	−0.32	0.19	0.00	0.05	0.23	−0.15	0.38
2) Jul Asian 200-mb geopotential height	−0.18	—	0.35	−0.28	−0.01	−0.19	−0.29	0.16	−0.23
3A–3B) Jul–Aug Atlantic 1000-mb *U*	−0.32	0.35	—	−0.22	−0.08	−0.28	−0.35	0.13	−0.24
4) Feb W African 1000-mb *U*	0.19	−0.28	−0.22	—	−0.18	−0.09	0.06	−0.09	0.15
5) Apr NE Siberian 200-mb *U*	0.00	−0.01	−0.08	−0.18	—	−0.07	0.18	−0.11	−0.12
6) Aug Indonesian SLP	0.05	−0.19	−0.28	−0.09	−0.07	—	0.16	0.01	0.18
7) Aug S Indian Ocean SLP	0.23	−0.29	−0.35	0.06	0.18	0.16	—	−0.14	0.09
8) May central African 200-mb *V*	−0.15	0.16	0.13	−0.09	−0.11	0.01	−0.14	—	−0.42
9) Jan–Feb W Pacific 200-mb *U*	0.38	−0.23	−0.24	0.15	−0.12	0.18	0.09	−0.42	—
Avg intercorrelation	0.19	0.21	0.25	0.16	0.09	0.13	0.19	0.15	0.23

5. Physical links between predictors and September hurricanes

Many of the predictor relationships identified and utilized for this September forecast, though not previously known to be important in forecasting the full Atlantic basin tropical cyclone season, have nevertheless in combination strikingly large correlations with September TC activity. Establishing plausible physical links between the predictor and September hurricanes is important for a better understanding of the skill of this forecast. One method used to illuminate physical relationships was to correlate the predictor in question with September reanalysis fields. That way, one can see what September features are inhibited (or enhanced) based on the positive (or negative) values of the predictor. For example, if one sees that the predictor correlates strongly with cold sea surface temperatures in the eastern Pacific, the implicit relationship with ENSO can be investigated further. In the following discussion, hypothetical links between each predictor and September TC activity are discussed. The sign of the correlation between the predictor and increased September TC activity is listed in parentheses, and the predictors are discussed in the order they are listed in Table 4. Refer to Fig. 4 for the geographical location of each predictor.

a. April 1000-mb U (12.5°–30°S, 40°W–10°E) (−)

Easterly winds of 6–10 m s^{-1} are commonly found throughout this region in April. An increase in the strength of these easterlies is associated with increased trade winds in the Southern Hemisphere, reduced vertical wind shear in the tropical Atlantic, and a more active year for Atlantic hurricanes.

b. July 200-mb geopotential height (32°–42°N, 100°–160°E) (+)

High heights in this region extending from the Tibetan Plateau across Japan and into the Pacific Ocean seem to contain important information about the global circulation pattern. First, high heights imply warmer temperatures across mainland China, indicating that the Asian monsoon is likely already stronger than normal due to an increased land–sea temperature contrast (Krishnamurthy and Goswami 2000). Easterly anomalies at 200 mb throughout the Tropics, including the Atlantic, are also associated with an enhanced Asian monsoon due to anomalously high heights in the midlatitudes and anomalously low heights in the Tropics. In addition, higher heights in this particular region indicate that the zone of tropical easterlies is shifted northward in the Pacific Ocean. A northward shift of the easterlies in the Pacific indicates that La Niña conditions are likely prevalent.

c. July–August 1000-mb U (5°–15°N, 30°–50°W)–(22.5°–35°N, 35°–65°W) (+) (−)

Being located in the tropical Atlantic, this predictor probably has the clearest direct link to Atlantic basin

TABLE 9. Correlations between predictors and Sep values of global modes for the period 1950–2000. Average intercorrelations are computed without respect to sign. Definitions for the global modes used here are defined in the appendix.

Predictor	SOI	Niño-1 + 2	Niño-3	NIño-4	Niño-3.4	PDO	QBO	AO
1) Apr S Atlantic 1000-mb *U*	0.00	0.12	0.16	0.16	0.15	0.17	−0.14	−0.30
2) Jul Asian 200-mb geopotential height	0.21	−0.23	−0.30	−0.16	−0.27	−0.45	0.18	0.25
3A–3B) Jul–Aug Atlantic 1000-mb *U*	0.44	−0.44	−0.53	−0.55	−0.55	−0.58	0.01	0.33
4) Feb W African 1000-mb *U*	−0.06	−0.11	0.02	−0.01	0.05	0.07	−0.21	−0.12
5) Apr NE Siberian 200-mb *U*	−0.34	0.23	0.31	0.33	0.35	0.01	−0.18	0.08
6) Aug Indonesian SLP	−0.42	0.38	0.44	0.42	0.42	0.29	0.16	0.07
7) Aug S Indian Ocean SLP	−0.42	0.19	0.32	0.38	0.39	0.30	−0.05	−0.19
8) May central African 200-mb *V*	0.02	−0.13	−0.11	0.07	−0.05	−0.06	−0.05	−0.08
9) Jan–Feb W Pacific 200-mb *U*	−0.12	0.22	0.16	0.11	0.11	0.20	−0.05	−0.28
Avg intercorrelation	0.23	0.23	0.26	0.24	0.26	0.24	0.11	0.19

tropical cyclones. When trade winds in the tropical Atlantic have westerly anomalies, that is, the trade winds are weaker, the vertical shear is typically reduced, thereby enhancing the likelihood of TC development. Increased trades enhance the vertical shear causing displacement of the low-level and upper-level circulation, tilting the potential vorticity pattern in the vertical, and subsequently warming middle layers of the atmosphere. All of these effects inhibit organized deep convection (DeMaria 1996). The 1 September version of this predictor has two locations. The additional area component for the 1 September predictor is the intensity of the low-level wind in the subtropics. If these subtropical winds have easterly anomalies, and the trade winds have westerly anomalies, there is an implicit increase in low-level cyclonic vorticity. Preexisting low-level cyclonic vorticity is one of the primary ingredients necessary for development of easterly waves into tropical storms (Gray 1979). At the same time, weaker trade winds in July and August reduce surface fluxes from the sea, keeping the tropical Atlantic water warmer and feeding back into continued reduced trades in September.

d. February 1000-mb U (20°–30°N, 15°W–15°E) (−)

Increased easterly anomalies at this location are associated with increased anticyclonic vorticity across much of mainland Europe. These anomalies imply that the Azores high has shifted north of its usual location, a condition that Knaff (1998) suggests is linked to weaker trades and concurrent warmer Atlantic upper mixed layer temperatures. Weaker winter to spring trade winds reduce upwelling off the west African coastline thereby helping to keep ocean surface layer temperatures warm, leading to above-average sea surface temperatures during the summer. As noted earlier, weaker trades and warmer Atlantic sea surface temperatures are favorable for September TC activity.

e. April 200-mb U (67.5°–85°N, 110°–180°E) (−)

The zonal wind in the polar region in northeast Siberia is probably the most difficult predictor to associate with September TC activity. Weaker westerlies in this region are one of the signatures of a weak Arctic Oscillation (AO) as documented in Thompson and Wallace (2000). The Arctic Oscillation and North Atlantic Oscillation (NAO) are correlated quite strongly, and a low NAO index implies more blocking in the North Atlantic. Blocking in the North Atlantic occurs more frequently with warm North Atlantic sea surface temperatures, as modeled by Rodwell et al. (1999), and a warm North Atlantic implies a stronger thermohaline circulation, which is favorable for more September TC activity.

f. August SLP (0°–30°S, 120°–160°E) (−)

Sea level pressure in this region in August correlates strongly with all ENSO indices ($r \sim |0.4|$) and the Southern Oscillation index (SOI). The SOI was first documented by Sir Gilbert Walker in the early part of the twentieth century during his seminal research in global-scale teleconnection patterns (Walker 1923, 1924, 1928), and this seesaw in sea level pressure anomalies between Darwin, Australia, and Tahiti has been well documented by other researchers as well, such as Bjerknes (1969), Rasmusson and Carpenter (1982), and Larkin and Harrison (2001). Low pressure in the Papua New Guinea–northern Australia region is indicative of a strong SOI, and this correlates strongly with cool September Niño-3.4 conditions and enhanced Atlantic TC activity.

g. August SLP (20°–45°S, 60°–90°E) (−)

Low sea level pressure in this region also correlates quite strongly ($r \sim |0.35|$) with the SOI and indexes involving Niño-3 and -4. Increased trades in the Pacific and heightened easterlies in the Atlantic are associated with low pressure in the southern Indian Ocean. This pressure index provides different information than the pressure index used for predictor 6 since, as was found in Wright et al. (1988), pressure anomalies in this region propagate toward Darwin, Australia, in only 1 or 2 months. Therefore, if the pressure area in the predictor 7 area is high and the pressure in the predictor 6 area is low, the Southern Oscillation index may be switching from high to neutral or low, and therefore a shift in ENSO may be occurring. If low pressure extends all the way from Australia to near the coast of Africa, then a strong La Niña event is likely taking place indicating increased TC activity in the Atlantic.

h. May 200-mb V (0°–20°S, 15°–30°E) (+)

The May 200-mb V over central Africa was also found to have a significant relationship with ENSO according to hypothetical modeling studies. Cook (2001) found that an Eastern Hemispheric wave developed when modeling an ENSO event as the Walker circulation weakens and shifts eastward. This development causes anomalous convergence to develop off the southeast coast of Africa, inducing northerly flow over central Africa and southerly flow centered over Madagascar. Therefore, southerly flow over central Africa likely indicates cool ENSO conditions, which is generally favorable for more TC activity in the Atlantic. Although this feature appears in modeling results of ENSO, significant correlations between September ENSO conditions and this predictor do not appear in Table 9. One other possible mechanism linking this predictor to September TC activity is that the circulation over central Africa has something to do with the easterly wave setup that is beginning to establish itself at this time of year.

TABLE 10. Ratio of top 10–bottom 10 years for all predictors in the 1 Sep forecast scheme.

Name of predictor	NS	NSD	H	HD	IH	IHD	TONS	TOH	NTC	Mean
1) Apr S Atlantic 1000-mb *U*	1.15	1.42	1.40	1.76	3.33	6.13	2.15	2.88	2.25	2.50
2) Jul Asian 200-mb geopotential height	1.46	1.80	2.20	2.10	4.40	3.51	2.29	3.50	2.49	2.64
3A–3B) Jul–Aug Atlantic 1000-mb *U*	1.64	2.19	2.36	3.70	3.83	10.77	2.83	6.00	3.47	4.09
4) Feb W African 1000-mb *U*	1.39	1.67	1.67	2.60	1.78	3.72	1.44	1.75	2.10	2.01
5) Apr NE Siberian 200-mb *U*	1.63	1.60	1.35	1.53	1.78	1.98	1.93	1.89	1.67	1.71
6) Aug Indonesian SLP	1.52	1.65	1.47	1.67	1.33	0.82	1.61	1.75	1.37	1.47
7) Aug S Indian Ocean SLP	1.63	1.31	2.31	1.53	2.00	2.02	1.56	2.63	1.78	1.86
8) May central African 200-mb *V*	1.33	1.77	1.93	2.72	1.78	3.32	1.63	1.82	2.14	2.05
9) Jan–Feb W Pacific 200-mb *U*	1.18	1.47	1.32	1.68	2.22	3.92	1.81	2.08	1.88	1.95
Mean	1.44	1.65	1.78	2.14	2.49	4.02	1.92	2.70	2.13	2.25

i. January–February 200-mb U (15°–25°N, 120°E–160°W) (−)

Easterly anomalies at 200 mb across this area of the Pacific correlate quite strongly with September La Niña conditions in the tropical Pacific. Anomalous easterlies at 200 mb in this location are associated with an anomalously broad upper-level anticyclone extending from off the coast of Japan to the eastern Pacific. In addition, negative values of this predictor are strongly correlated ($r > 0.5$) with a positive January–February SOI, which is well associated with stronger trade winds across the eastern and central Pacific. Stronger trade winds across the east and central Pacific are typical of La Niña conditions, which are favorable for Atlantic TC development.

These predictors were selected instead of simply utilizing large-scale indexes such as ENSO, the PDO, and the AO because the entire atmosphere–ocean circulation responds differently to a particular event, and the regions discussed above are apparently of critical importance in determining September TC activity in the Atlantic based upon the 51-yr period of hindcasting from 1950 to 2000. Physical relationships between predictors and predictands are still in their developmental stages and will be further explored through analysis of the newly available 40-yr ECMWF reanalysis and through further correlation-compositing studies. The physical linkages previously discussed are critical for explaining why the particular predictors were chosen for the September forecast; however, objective analysis of the statistical significance is also important.

6. Statistical significance testing

As discussed in the last section, some of the physical links between predictors and September tropical cyclone activity are easily explained while others are more challenging. The predictors selected for use in the forecast scheme were chosen because they explained a large amount of the variance in September TC activity. In addition, some of the predictors that were chosen correlated only moderately with September TC activity ($r \sim |0.3|$) but had statistically significant partial correlations after the most important predictors were already included in the forecasting scheme. Predictors 2 and 3 were chosen from the composite and correlation analysis only, predictors 1, 4–7, and 9 were chosen by examining both correlation and residual analysis simultaneously, and predictor 8 was chosen solely on the residual analysis. Such an approach raises the prospect that this is largely a massive effort in curve fitting with comparatively little actual physical linkage between many of the predictors chosen and TC activity; however, correlation relationships lead one to discover physical processes that might not have been examined without the initial correlation relationship.

Several objective statistical methods were used to test the likelihood that the predictors selected represent legitimate physical processes at work in the reanalysis data field. The first method considers the top 10 yr and bottom 10 yr of each predictor (mentioned in section 3) and checks to make sure that there is a sizable ratio between the top 10 and bottom 10 values. For example, one could take the ratio of named storms occurring with the 10 highest values of sea level pressure in a particular region and divide it by the number of named storms occurring with the 10 lowest values of sea level pressure in a particular region to obtain the ratio. As was expected, sizable ratios between predictors and September TC activity were obtained when the top 10–bottom 10 values were determined for each predictor. Table 10 displays these top 10–bottom 10 ratios. Note the large ratios for intense hurricane days and NTC. In addition, some of the ratios may not be large because teleconnection points are not always mirror images of each other. That is, the Atlantic may have increased hurricane activity with low sea level pressure in an area; however, average hurricane activity may be observed during high pressure years in the same area. Teleconnection atlases have shown that positive and negative phases of an index often have different geographical configurations, and further research is being done to see if this is the case with some of the Atlantic hurricane predictors.

Another quantitative way to test whether the predictors selected embody true skill is to subdivide the data. By splitting the 51-yr hindcast period into 1950–75 and 1976–2000, one can check to make sure that the correlation is of the same sign and similar magnitude

TABLE 11. Correlations between NTC and forecast predictors subdivided into 1950–75 and 1976–2000.

Predictor	1950–75 correlation	1976–2000 correlation	1950–2000 correlation	Correlation difference	% difference
1) Apr S Atlantic 1000-mb *U*	−0.50	−0.35	−0.43	0.15	35
2) Jul Asian 200-mb geopotential height	0.59	0.48	0.54	0.11	20
3A–3B) Jul–Aug Atlantic 1000-mb *U*	0.65	0.67	0.64	0.02	3
4) Feb W African 1000-mb *U*	−0.61	−0.15	−0.38	0.46	121
5) Apr NE Siberian 200-mb *U*	−0.16	−0.42	−0.29	0.26	90
6) Aug Indonesian SLP	−0.16	−0.23	−0.23	0.07	30
7) Aug S Indian Ocean SLP	−0.36	−0.37	−0.37	0.01	3
8) May central African 200-mb *V*	0.55	0.49	0.49	0.06	12
9) Jan–Feb W Pacific 200-mb *U*	−0.63	−0.30	−0.48	0.33	69

throughout the period. This technique helped to eliminate relationships that may have explained large amounts of variance in a residual analysis but whose relationships with September TC activity were not present in various portions of the dataset. Table 11 contains the correlations with NTC for both 1950–75 and 1976–2000. As one can see from Table 11, there are rather large correlation changes between time periods for predictors 4, 5, and 9. Since the correlations for predictors 4 and 5 are reduced considerably below the 95% level of statistical significance during the later and earlier time period, respectively, they are subjected to further testing outlined later in this section. Also, these predictors will be scrutinized to see if they show skill in independent forecasts issued over the next few years.

A method used to check the statistical significance of the forecast equation as a whole was done utilizing Miller's equivalent *F* test (Neumann et al. 1977). Utilizing a simple *F* test would considerably overestimate the statistical significance of the forecast equations since a total of 126 variables were considered for inclusion in the forecast technique. Therefore, Miller proposed that to calculate the *F* value necessary for statistical significance, the total number of variables examined must be included. The equation proposed for the 99% significance level was as follows:

$$F_{99} = F_{(1-1/100k)}, \tag{1}$$

where k is the total number of predictors screened for analysis. In this case, the total number of predictors is 126, and the level needed for statistical significance is $F_{0.99992}$. Table 12 displays the calculated *F* values needed for 99% significance based on Eq. (1) along with the actual *F* values for the individual forecast equations based on 51 yr of hindcasting. All forecast equations are significant at the 99% level excluding named storms hindcast on 1 August.

TABLE 12. Miller equivalent *F* test results for all forecast equations issued on 1 Aug and 1 Sep.

Predictor	51-yr *F* value	Miller F_{99}	Significant 99% level
1 Aug NS	6.63	9.02	No
1 Aug NSD	10.76	6.85	Yes
1 Aug H	9.51	9.02	Yes
1 Aug HD	13.53	6.85	Yes
1 Aug IH	15.54	6.85	Yes
1 Aug IHD	19.69	7.68	Yes
1 Aug TONS	11.34	7.68	Yes
1 Aug TOH	19.46	7.68	Yes
1 Aug NTC	26.86	6.85	Yes
1 Sep NS	7.32	6.85	Yes
1 Sep NSD	15.29	6.85	Yes
1 Sep H	9.65	7.68	Yes
1 Sep HD	18.24	6.85	Yes
1 Sep IH	15.23	6.85	Yes
1 Sep IHD	18.58	7.68	Yes
1 Sep TONS	9.44	6.85	Yes
1 Sep TOH	14.74	7.68	Yes
1 Sep NTC	27.46	6.85	Yes

A fourth quantitative method of checking the statistical significance of the data field was conducted by utilizing a simple Student's *t* test. Since hindcasts are based on a 51-yr time series, there are 50 degrees of freedom in the time series. Most of the relationships were discovered a posteriori; that is, the relationship was not expected prior to its inclusion in the forecast, and therefore two-tailed tests of statistical significance were conducted for all predictors except predictors 3 and 6. Trade wind strength in the tropical Atlantic (Gray 1968) and low sea level pressure in the Australia region (Gray et al. 2002) have both been documented in previous studies to impact seasonal tropical cyclone activity in the Atlantic, and therefore there was an a priori expectation that predictors 3 and 6 would effect Atlantic hurricanes. For all predictors, the actual statistical significance level needed was taken by computing the statistical significance level desired raised to the power of the number of predictors screened for analysis (126 possible predictors). To obtain the 95% significance level, one must calculate what value when taken to the 126th power will give you 0.95 (Wilks 1995). The critical correlation coefficient value associated with the 95% (99%) significance level for a two-sided test of significance of a posteriori correlation values with 50 degrees of freedom is 0.47 (0.51). Predictors 3 and 6 were expected a priori, and therefore the critical values for the one-tailed Student's *t* test were used; these values are 0.45 and 0.49 for the 95% and 99% significance levels, respectively. Table 13 identifies in italics (bold) those correlation coefficients that exceed the critical values for the 95% (99%) significance level associated with

TABLE 13. The 95% significance level as determined by the Student's *t* test is highlighted in italics, and the 99% significance level as determined by the Student's *t* test is highlighted in boldface. Correlations not significant at the 95% level are neither in italics nor bold.

Predictor	NS	NSD	H	HD	IH	IHD	TONS	TOH	NTC
1) Apr S Atlantic 1000-mb *U*	−0.21	−0.20	−0.27	−0.22	*−0.47*	*−0.48*	−0.30	−0.35	−0.43
2) Jul Asian 200-mb geopotential height	0.37	*0.48*	*0.47*	0.44	**0.56**	0.38	*0.50*	**0.53**	**0.54**
3A–3B) Jul–Aug Atlantic 1000-mb *U*	0.31	*0.47*	*0.45*	**0.58**	**0.56**	**0.58**	**0.49**	**0.61**	**0.64**
4) Feb W African 1000-mb *U*	−0.20	−0.34	−0.23	−0.42	−0.23	−0.37	−0.15	−0.16	−0.38
5) Apr NE Siberian 200-mb *U*	−0.31	−0.32	−0.21	−0.27	−0.23	−0.19	−0.27	−0.21	−0.29
6) Aug Indonesian SLP	−0.34	−0.35	−0.30	−0.26	−0.18	−0.04	−0.33	−0.36	−0.23
7) Aug S Indian Ocean SLP	−0.45	−0.25	*−0.50*	−0.27	−0.35	−0.22	−0.35	−0.43	−0.37
8) May central African 200-mb *V*	0.30	0.44	0.34	*0.47*	0.39	0.42	0.35	0.31	*0.49*
9) Jan–Feb W Pacific 200-mb *U*	−0.04	−0.33	−0.22	−0.35	−0.45	**−0.54**	−0.33	−0.37	*−0.48*

the Student's *t* test. Table 14 displays only correlation coefficients for predictors actually used to forecast a particular TC parameter. It should be noted that although some of the individual predictor–Atlantic tropical cyclone parameter relationships are not statistically significant, the equivalent Miller *F* test discussed above shows that all hindcast equations except named storm days hindcast on 1 August are significant at the 99% level. Therefore, the power of these predictors is not in their individual correlations with tropical cyclone activity but in their combined use with the other predictors in the scheme.

The two predictors that looked most questionable in terms of the stability and strength of correlation over the 51-yr hindcasting period were subjected to further testing. The February 1000-mb *U* over West Africa and the April 200-mb *U* in NE Siberia were evaluated further by first examining the probability density function of correlations between randomly selected 25-yr periods in the dataset and NTC. In this case, one thousand 25-yr subset periods were generated to see if the 51-yr correlation for the predictor fell approximately in the center of the distribution. Figures 7 and 8 display the probability density functions for the West Africa 1000-mb *U* and the NE Siberia 200-mb *U*, respectively. The 51-yr correlations of both predictors fell close to the middle of the probability density function of the randomly selected 25-yr subsets, which adds confidence to their use in the forecast scheme. Please note that the randomly selected 25-yr subsets did not frequently fall in the tails of the distribution.

An additional test that was conducted on the two most questionable predictors was to see the stability of month-by-month correlations between the predictor and September NTC. The correlation between monthly values of these two predictors and September NTC was first calculated for the entire 51-yr time series, and then the time series was broken up into 1950–75 and 1976–2000 to see how much variability there was in the correlations. Figures 9 and 10 show the month-to-month correlations between predictors 4 and 5, respectively, and September NTC for 1950–2000, 1950–75, and 1976–2000. In general, the correlation trend observed in the month used to hindcast September NTC is similar to the trend of the year as a whole. For example, West Africa 1000-mb *U* has increased negative correlations for all months except October and November when evaluating the 1950–75 subset. A close watch will be kept on these predictors to evaluate their utility in the September forecast. In addition, when issuing real-time September forecasts, these predictors are given less weight than the other more stable predictors in the forecast scheme.

7. Forecast applications

a. September U.S. tropical cyclone landfalling probability forecast

An important element of the September forecast is the issuing of probability forecasts for U.S. landfalling tropical cyclones. September landfalling tropical cyclones can be quite devastating as one just has to recall the damage and devastation from such powerful storms as Hurricanes Fran and Hugo. Intense hurricanes are of special importance since they cause approximately 85%

TABLE 14. As in Table 13 but correlation coefficients are only displayed for predictors actually used to forecast a particular TC parameter.

Predictor	NS	NSD	H	HD	IH	IHD	TONS	TOH	NTC
1) Apr S Atlantic 1000-mb *U*	—	—	—	—	*−0.47*	—	—	—	—
2) Jul Asian 200-mb geopotential height	—	*0.48*	*0.47*	—	**0.56**	—	*0.50*	**0.53**	**0.54**
3A–3B) Jul–Aug Atlantic 1000-mb *U*	—	—	*0.45*	**0.58**	**0.56**	**0.58**	**0.49**	**0.61**	**0.64**
4) Feb W African 1000-mb *U*	−0.20	−0.34	—	−0.42	—	−0.37	—	—	−0.38
5) Apr NE Siberian 200-mb *U*	−0.31	−0.32	—	−0.27	−0.23	−0.19	−0.27	−0.21	−0.29
6) Aug Indonesian SLP	−0.34	−0.35	—	−0.26	—	—	−0.33	—	—
7) Aug S Indian Ocean SLP	−0.45	—	*−0.50*	—	—	—	—	—	—
8) May central African 200-mb *V*	0.30	0.44	0.34	*0.47*	0.39	—	0.35	—	*0.49*
9) Jan–Feb W Pacific 200-mb *U*	—	—	—	—	—	**−0.54**	—	−0.37	—

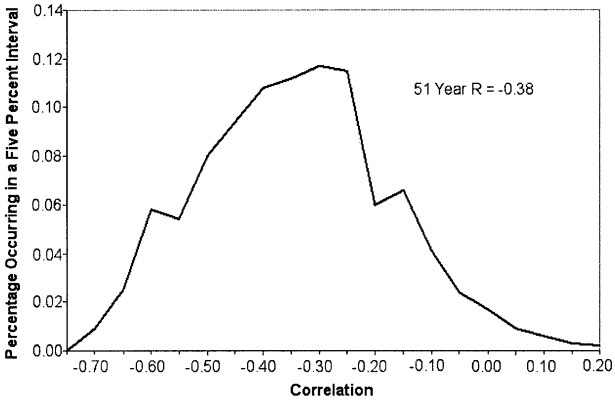

FIG. 7. Probability density function of correlations between 1000 randomly selected 25-yr subsets of Feb West Africa 1000-mb *U* (predictor 4) and NTC.

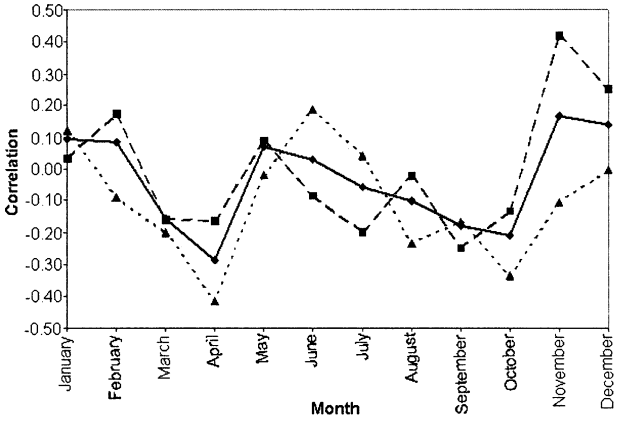

FIG. 9. Monthly correlations (*r*) between West Africa 1000-mb *U* (predictor 4) and Sep NTC. The solid line represents the entire time series of 1950–2000, the long dashed line represents 1950–75, and the short dashed line represents 1976–2000.

of all TC damage when normalized for population and wealth per capita (Pielke and Landsea 1998). Although on a year-to-year basis it is impossible to forecast a landfalling storm, there is a definite increase in probability of landfall during active years. One way to demonstrate the increase in probability of landfall with increased NTC is to rank years by hindcast NTC and then correlate the number of U.S. landfalling tropical cyclones with hindcast NTC. For an individual year, the correlation between U.S. landfalling hurricanes and hindcast NTC is only 0.38. However, if one computes a 5-yr moving average of hindcast NTC and a 5-yr moving average of the number of landfalling storms, the correlation improves to 0.77. Figure 11 displays the improvement in correlation between hindcast NTC and landfalling hurricanes when a moving average is applied to the data.

The utility of landfall probabilities can also be seen by examining landfall differences between high and low observed and hindcast years. For example, there was only one hurricane and no intense hurricanes that made landfall during the 15 lowest observed values of September NTC; however, there were 17 hurricanes and 7 intense hurricanes that made landfall during the 15 highest observed values of September NTC. Hindcast values of September NTC provide similar striking landfall contrasts. Only 1 major hurricane and 3 total hurricanes made landfall during the 15 lowest hindcasts of September NTC; whereas, the 15 highest years of hindcast NTC had 13 hurricanes and 6 intense hurricanes make landfall. Figure 12 displays the hurricane landfalls that took place during the 15 highest and 15 lowest September NTC hindcasts, respectively. One can tell from these maps that forecast values of NTC indicate a higher or lower probability of landfall along the United States coast.

Separate equations were calculated based on both forecast and actual values of NTC, and the equations developed from the actual NTC were found to be more representative of actual landfall events. Equations were derived by ranking years from highest to lowest in NTC

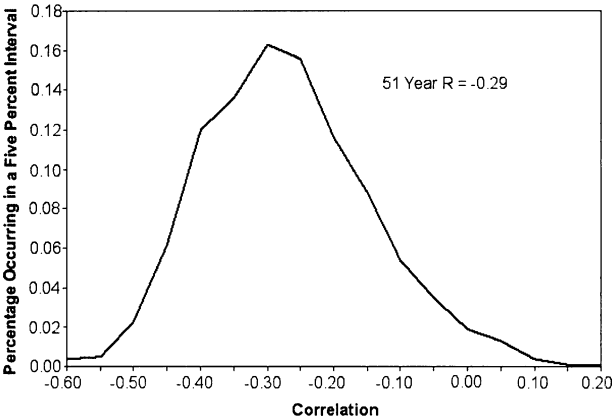

FIG. 8. Probability density function of correlations between 1000 randomly selected 25-yr subsets of Apr NE Siberia 200-mb *U* (predictor 5) and NTC.

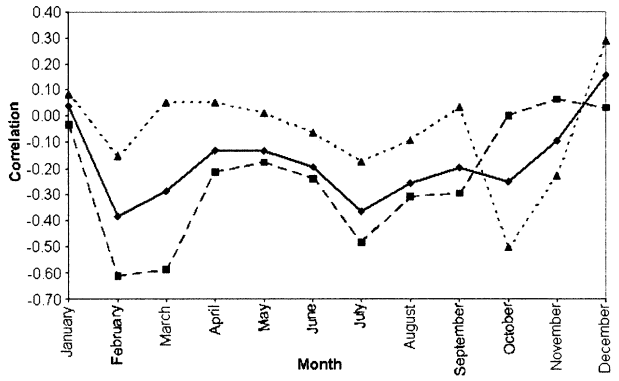

FIG. 10. Monthly correlations (*r*) between NE Siberia 200-mb *U* (predictor 5) and Sep NTC. The solid line represents the entire time series of 1950–2000, the long dashed line represents 1950–75, and the short dashed line represents 1976–2000.

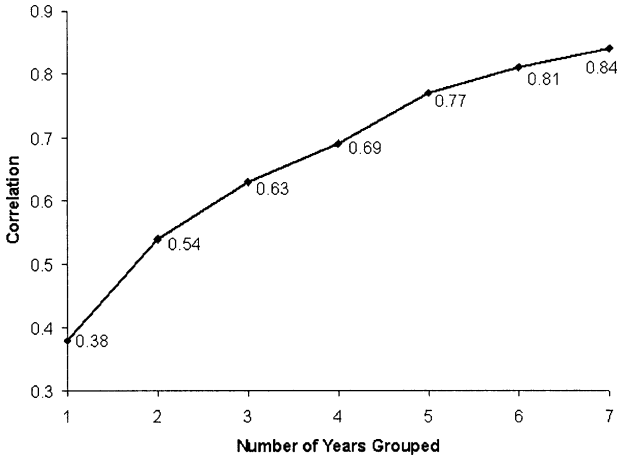

FIG. 11. Improvement in the correlation between hindcast landfall probability and U.S. landfalling hurricanes when several years of landfalling activity and landfalling probabilities are grouped together.

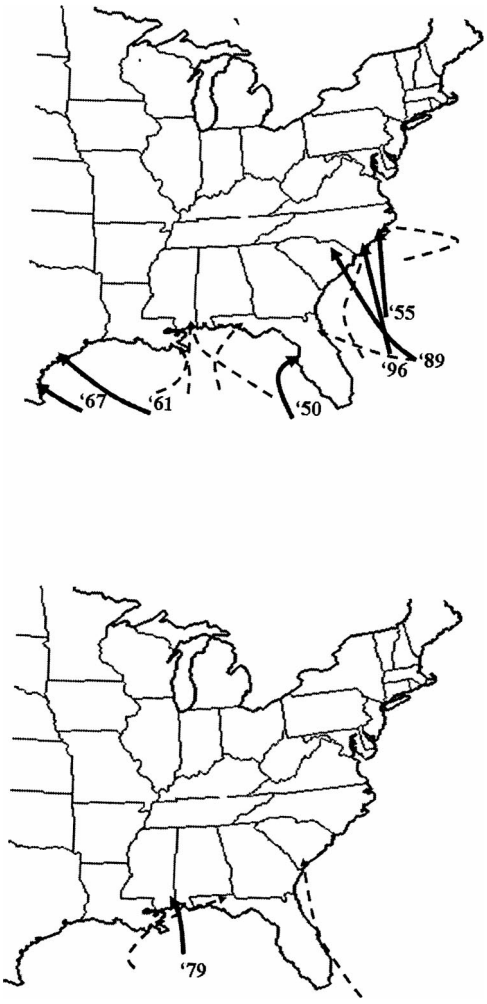

FIG. 12. Landfalling tropical cyclones during the 15 highest Sep NTC hindcasts issued on 1 Aug and the 15 lowest Sep NTC hindcasts issued on 1 Aug. Category 1–2 hurricanes are the dashed lines while category 3–5 hurricanes are the solid lines. Years of landfalling intense hurricanes are as indicated.

and then subdividing the data into halves, thirds, and fourths. Average NTC values for each half, third, and fourth of the data were calculated along with the probability of landfalling named storms, hurricanes, and intense hurricanes during those years. After the average NTC and probability calculations were made, a simple linear least squares equation was developed that calculated probability as a function of NTC. Table 15 displays the U.S. landfall probability hindcasts issued on 1 August for tropical cyclones, hurricanes, and intense hurricanes for 1950–2000 along with the landfalling statistics for those years. Table 16 compares the number of years with at least one U.S. landfalling tropical cyclone for the top 5 and bottom 5, the top 10 and bottom 10, and the top 15 and bottom 15 landfall probability hindcasts, respectively, issued on 1 August. In general, years with high landfall probabilities are more likely to have a tropical cyclone strike the U.S. coast. Equations (2)–(4) below display the landfalling equations for named storms, hurricanes, and intense hurricanes, respectively. It should be noted that, based on these equations, if the value of NTC were large enough, the probability of landfall would exceed 100%. In this case, the probability would be set to 99% since it is never a given that a storm will make landfall in any particular month:

$$\text{Named Storm Probability} = 34.62 + 0.67(\text{NTC}), \quad (2)$$

$$\text{Hurricane Probability} = 5.09 + 0.92(\text{NTC}), \quad (3)$$

$$\text{Intense Hurricane Probability} = 5.12 + 0.50(\text{NTC}). \quad (4)$$

b. Improvement of Atlantic basin tropical cyclone seasonal forecast

Gray has been issuing seasonal forecasts since 1984. We find that some improvement to the NTC forecast can be made by modifying Gray's hindcast (prior to 1984) and forecast (since 1984) NTC values by the September NTC hindcast issued on 1 August. September NTC values were modified slightly from the 1950–2000 climatology to the 1950–1990 climatology to be in keeping with the NTC hindcast/forecast values calculated by Gray. The changing of the climatological baseline generally increased September NTC values by 3%–5%. By assuming that September composes 50% of the post–1 August hurricane season and consequently weighting the September NTC hindcast as 50% of the forecast NTC and counting Gray's original forecast as the other 50%, the nonjackknifed variance explained increases from 57% to 74%. In addition, by adding Blake's (2002) August hindcast NTC predictions and assuming that August accounts for 25% of the season and reducing the weighting of Gray's original forecast to 25%, the nonjackknifed variance explained in the post–1 August fore-

TABLE 15. The 1 Aug hindcast landfall probabilities (Prob.) issued for 1950–2000 along with the actual observed landfalls for those years.

Year	Prob. NS	Prob. H	Prob. IH	Landfalling NS	Landfalling H	Landfalling IH
1950	92.0	83.9	47.9	1	1	1
1951	72.6	57.2	33.4	0	0	0
1952	76.9	63.1	36.6	0	0	0
1953	87.8	78.1	44.8	3	2	0
1954	54.2	32.0	19.8	1	1	1
1955	92.1	84.0	48.0	1	1	1
1956	48.3	23.8	15.3	1	1	0
1957	72.0	56.5	33.1	2	0	0
1958	67.8	50.6	29.9	1	0	0
1959	68.7	51.9	30.6	1	1	1
1960	77.8	64.4	37.4	2	2	1
1961	122.7	126.1	70.9	2	1	1
1962	59.6	39.4	23.7	0	0	0
1963	73.6	58.6	34.2	1	1	0
1964	83.7	72.5	41.8	1	1	0
1965	51.2	27.8	17.5	1	1	1
1966	66.0	48.2	28.5	0	0	0
1967	79.3	66.5	38.5	2	2	1
1968	48.5	24.1	15.4	0	0	0
1969	64.7	46.4	27.6	1	1	0
1970	58.3	37.5	22.8	1	0	0
1971	60.8	41.0	24.6	3	3	0
1972	37.1	8.5	7.0	0	0	0
1973	55.3	33.5	20.6	1	0	0
1974	64.7	46.4	27.6	1	1	1
1975	77.8	64.4	37.4	1	1	1
1976	53.6	31.1	19.3	0	0	0
1977	50.5	26.9	17.0	1	1	0
1978	64.0	45.4	27.0	0	0	0
1979	47.6	22.9	14.8	3	2	1
1980	66.5	48.8	28.9	1	0	0
1981	80.9	68.6	39.6	0	0	0
1982	34.5	5.0	5.1	1	0	0
1983	48.1	23.6	15.2	1	0	0
1984	66.9	49.4	29.2	2	1	1
1985	60.0	39.9	24.1	2	2	2
1986	42.9	16.4	11.3	0	0	0
1987	63.6	44.9	26.8	0	0	0
1988	82.1	70.3	40.6	1	1	0
1989	86.0	75.6	43.4	1	1	1
1990	57.9	37.0	22.5	0	0	0
1991	39.6	12.0	8.9	0	0	0
1992	52.7	29.9	18.6	1	0	0
1993	61.3	41.7	25.0	0	0	0
1994	59.4	39.2	23.6	0	0	0
1995	83.2	71.8	41.4	0	0	0
1996	69.1	52.4	30.9	1	1	1
1997	56.6	35.3	21.5	0	0	0
1998	79.1	66.2	38.4	3	2	0
1999	92.6	84.7	48.4	3	1	0
2000	75.3	61.0	35.5	2	0	0

cast increases to 83%. Equation (5) below shows the formula used to obtain the revised seasonal forecast:

$$\text{Seasonal NTC} = \text{Aug. NTC} + \text{Sep. NTC} + [(0.25)(\text{Gray Seasonal NTC})]. \quad (5)$$

Table 17 displays Gray's forecast 1 August NTC, the new 1 August NTC forecast modified by both the September hindcast and Blake's August hindcast, the actual NTC, the residual assuming climatology, the original residual of Gray's seasonal forecast, and the new residual based on the modified forecast with both the August and September hindcasts included. Average residual values are reduced by more than 25% for the period of 1950–2000 when both the August and September hindcasts are considered in the seasonal forecast.

8. Conclusions and future work

a. Conclusions

Utilizing NCEP–NCAR reanalysis data, a September Atlantic basin tropical cyclone forecast has been de-

TABLE 16. Number of years with at least one landfalling tropical cyclone for the top 5 and bottom 5, top 10 and bottom 10, and top 15 and the bottom 15 1 Aug hindcast landfall probabilities.

Hindcast landfall probability	NS	H	IH
5 highest	5	5	3
5 lowest	2	1	1
Ratio (as %)	250	500	300
10 highest	8	8	5
10 lowest	6	4	2
Ratio (as %)	133	200	250
15 highest	12	12	7
15 lowest	9	5	3
Ratio (as %)	133	240	233

veloped that shows considerable skill in hindcasting based on 51 yr of data (1950–2000). Up to 75% of the variance in tropical cyclone activity can be hindcast 1 month in advance. September forecast predictors are global in nature and utilize reanalysis ''A'' variables, which, according to Kalnay et al. (1996), are the most reliable in the reanalysis dataset. The most important predictor for September TC activity in the Atlantic is the strength of the July–August trade winds in the tropical Atlantic. Other predictors relate strongly to global modes such as ENSO or the PDO; however, several predictors do not relate strongly to any global modes. The methodology of this forecast utilizes correlation relationships (i.e., linear relationships) similar to those utilized by other seasonal tropical cyclone forecasting groups such as the National Oceanic and Atmospheric Administration/National Hurricane Center (NOAA/NHC; information available online at http://www.nhc.noaa.gov) and Tropical Storm Risk (information available online at http://www.tropicalstormrisk.com). Empirical relationships were utilized to develop the forecast, and these relationships can lead to important new research directions that would otherwise not be followed. The empirical approach, as opposed to the numerical approach, often leads to the best answers for seasonal and climate prediction. In addition, the utilization of the statistical approach can provide clues to improve understanding of physical processes.

Forecasts of September TC activity will be issued annually on 1 August with an update issued on 1 September. The September Atlantic basin hurricane forecast will hopefully provide skillful advanced information on Atlantic TC activity that may be useful for emergency planners and coastal residents alike.

See the project report by Klotzbach (2002) for more background information on the September forecast and the project report by Blake (2002) for more background information on the August forecast of Atlantic basin TC activity.

b. Future work

Although the Atlantic basin September TC forecast shows considerable hindcast skill, there are still many areas for future work. The forecast methodology was based on 51 yr of hindcasting utilizing NCEP–NCAR reanalysis data. In addition to the NCEP–NCAR reanalysis dataset used to make this forecast, the ECMWF has been undertaking a reanalysis project that will soon be available to the scientific and forecasting community. The ability to compare the hindcasting ability of the forecast technique utilizing two different reanalysis schemes would be of considerable value. If the forecast technique worked equally or possibly even more effectively on the ECMWF reanalysis, it would lend confidence to the soundness of physical linkages between predictors and September TC activity since the data assimilated and the model used in the ECMWF reanalysis are different from those used in the NCEP–NCAR reanalysis. Also, agreement between the ECMWF and NCEP–NCAR reanalyses would provide greater assurance of the utility of the reanalysis products.

Seasonal forecasts similar to those currently being issued by operational centers such as NCEP could be developed utilizing the methodology outlined in this paper. In addition, other weather events such as ENSO, cold outbreaks, and blocking patterns in the Atlantic and Pacific should be investigated to determine if there is similar significant forecasting ability for these phenomena. A skillful forecast of ENSO would be of great value to people around the world. ENSO's effects are felt globally as was documented by Sir Gilbert Walker many years ago (Walker 1923, 1924, 1928), and some of its realizations include flooding, drought, heat, and cold-air outbreaks. With the recent availability of the NCEP reanalysis, there is now a plethora of global data to enhance further study and forecasting of ENSO that was not available when Walker was conducting his famous teleconnection studies. A long-lead forecast of ENSO would allow individuals time to prepare for ENSO's effects in their part of the world.

Reanalysis products have allowed for easy access to global datasets that were not previously available. The hindcast skill of both this scheme and the August forecast scheme indicate that there is likely similar hindcast skill for forecasting October TC activity. If an accurate scheme is developed for October, then a seasonal forecast could be issued based on the August, September, and October forecasts. One could then compare this seasonal forecast to the seasonal forecast currently issued by Gray and colleagues to see if there is a close agreement between the two forecasts. The early (June–July) and late (November) parts of the hurricane season present a more difficult forecasting challenge. Early and late season storms often form from baroclinic systems such as cold lows or along the trailing edges of fronts, and these midlatitude phenomena are very difficult to predict months in advance. Perhaps probability forecasts for early and late season activity could be issued in a way similar to the way that current landfall probability forecasts are issued.

All statistical forecast schemes are based on the idea

TABLE 17. Original 1 Aug Gray hindcast values of NTC, Aug and Sep forecast modified values of NTC, actual NTC values, residual assuming climatology, original forecast residual, and the new residual based on the modified forecast.

Year	Seasonal NTC after 1 Aug	Blake Aug NTC hindcast	Sep NTC hindcast	Gray et al. after 1 Aug forecast	New Gray et al. after 1 Aug forecast	Residual assuming climatology	Old residual	New residual
1950	237	62.9	89.5	149	189.7	137.0	88.0	47.3
1951	108	32.0	59.2	106	117.7	8.0	2.0	−9.7
1952	93	26.2	65.9	154	130.6	−7.0	−61.0	−37.6
1953	113	18.9	82.9	119	131.6	13.0	−6.0	−18.6
1954	116	3.0	30.6	119	63.4	16.0	−3.0	52.6
1955	192	68.1	89.7	163	198.6	92.0	29.0	−6.6
1956	60	31.8	21.3	137	87.4	−40.0	−77.0	−27.4
1957	66	6.5	58.4	88	86.9	−34.0	−22.0	−20.9
1958	135	67.3	51.7	141	154.3	35.0	−6.0	−19.3
1959	74	11.6	53.2	69	82.1	−26.0	5.0	−8.1
1960	82	7.6	67.4	100	100.0	−18.0	−18.0	−18.0
1961	209	10.4	137.4	189	195.1	109.0	20.0	13.9
1962	33	13.4	38.9	77	71.6	−67.0	−44.0	−38.6
1963	115	40.9	60.8	123	132.5	15.0	−8.0	−17.5
1964	159	40.7	76.6	162	157.8	59.0	−3.0	1.2
1965	82	4.8	25.8	42	41.1	−18.0	40.0	40.9
1966	95	31.1	49.0	160	120.1	−5.0	−65.0	−25.1
1967	96	5.1	69.7	65	91.1	−4.0	31.0	4.9
1968	24	8.2	21.6	5	31.1	−76.0	19.0	−7.1
1969	150	30.5	46.9	250	139.9	50.0	−100.0	10.1
1970	55	29.3	36.9	81	86.5	−45.0	−26.0	−31.5
1971	91	16.1	40.8	115	85.7	−9.0	−24.0	5.3
1972	20	14.7	3.8	38	28.0	−80.0	−18.0	−8.0
1973	43	13.4	32.3	86	67.2	−57.0	−43.0	−24.2
1974	75	24.3	46.9	84	92.2	−25.0	−9.0	−17.2
1975	81	34.5	67.4	93	125.2	−19.0	−12.0	−44.2
1976	81	38.9	29.5	75	87.2	−19.0	6.0	−6.2
1977	46	5.3	24.7	45	41.3	−54.0	1.0	4.7
1978	83	23.0	45.8	86	90.3	−17.0	−3.0	−7.3
1979	84	40.9	20.2	63	76.9	−16.0	21.0	7.1
1980	134	53.8	49.7	137	137.8	34.0	−3.0	−3.8
1981	108	17.4	72.1	138	124.0	8.0	−30.0	−16.0
1982	31	6.4	−0.1	40	16.3	−69.0	−9.0	14.7
1983	31	23.0	21.1	29	51.4	−69.0	2.0	−20.4
1984	77	13.5	50.3	67	80.6	−23.0	10.0	−3.6
1985	100	13.2	39.6	96	76.8	0.0	4.0	23.2
1986	29	15.9	12.9	65	45.1	−71.0	−36.0	−16.1
1987	47	24.0	45.3	47	81.1	−53.0	0.0	−34.1
1988	122	11.3	74.1	125	116.7	22.0	−3.0	5.3
1989	124	31.5	80.1	127	143.4	24.0	−3.0	−19.4
1990	89	52.0	36.3	142	123.8	−11.0	−53.0	−34.8
1991	56	27.6	7.8	70	52.9	−44.0	−14.0	3.1
1992	66	36.2	28.2	62	79.9	−34.0	4.0	−13.9
1993	51	25.9	41.5	54	80.9	−49.0	−3.0	−29.9
1994	34	8.6	38.7	45	58.6	−66.0	−11.0	−24.6
1995	205	64.4	75.8	166	181.7	105.0	39.0	23.3
1996	169	50.9	53.8	204	155.7	69.0	−35.0	13.3
1997	35	4.1	34.3	89	60.7	−65.0	−54.0	−25.7
1998	170	57.8	69.5	110	154.8	70.0	60.0	15.2
1999	193	55.7	90.4	130	178.6	93.0	63.0	14.4
2000	134	32.2	63.5	60	110.7	34.0	74.0	23.3
Avg	96.1	27.2	49.6	101.7	102.2	|42.8|	|25.9|	|18.8|

that the atmosphere's future behavior will be similar to its behavior in the past. If there is a large-scale atmospheric paradigm shift, the effects of which are not represented in the developmental data, then the forecasting ability of this forecast of September TC activity may fail to be useful. Nevertheless, this forecast scheme shows skill through the climate regime when the Atlantic thermohaline circulation was strong (1950–69, 1995–2000) and when it was weak (1970–94). The soundness of physical linkages is key in determining likely future forecast skill. Further research into many of the physical linkages will be continued for clearer explanations of the relationships between predictors and September hurricane activity.

Acknowledgments. We would like to thank Eric Blake and John Sheaffer for many helpful discussions on monthly tropical cyclone variability. We would also like to thank the three anonymous reviewers whose comments helped improve this manuscript. This research was supported by NSF Climate Grant ATM-0087398.

APPENDIX

List of Symbols and Acronyms

AO	Arctic Oscillation—the leading empirical orthogonal function (EOF) of sea level pressure poleward of 20°N based on all months from January 1958 to April 1997
CDC	Climate Diagnostics Center, Boulder, Colorado
ECMWF	European Centre for Medium-Range Weather Forecasts, Reading, United Kingdom
EN	El Niño—a 12–18-month period during which anomalously warm sea surface temperatures occur in the eastern half of the equatorial Pacific
ENSO	El Niño–Southern Oscillation
H	Hurricane—a tropical cyclone with sustained low-level winds of 74 mi h^{-1} (33 m s^{-1} or 64 kt) or greater
HD	Hurricane day—a measure of hurricane activity, one unit of which occurs as four 6-h periods during which a tropical cyclone is observed or estimated to have hurricane intensity winds
IH	Intense hurricane—a hurricane that reaches a sustained 1-min-average 10-m wind of at least 111 mi h^{-1} (50 m s^{-1} or 96 kt) at some point in its lifetime; this constitutes a category 3 or higher storm on the Saffir–Simpson scale (also termed a major hurricane)
IHD	Intense hurricane day—four 6-h periods during which a hurricane has intensity of Saffir–Simpson category 3 or higher
MJO	Madden–Julian oscillation
NAO	North Atlantic Oscillation—a normalized measure of the surface pressure difference between Ireland and Portugal
NCAR	National Center for Atmospheric Research, Boulder, Colorado
NCEP	National Centers for Environmental Prediction, Washington, D.C.
Niño-1 + 2	Sea surface temperatures in the region from 0° to 10°S and 90° to 80°W
Niño-3	Sea surface temperatures in the region from 5°N to 5°S and 150° to 90°W
Niño-3.4	Sea surface temperatures in the region from 5°N to 5°S and 170° to 120°W
Niño-4	Sea surface temperatures in the region from 5°N to 5°S and 160°E to 150°W
NS	Named storm—a hurricane or a tropical storm.
NSD	Named storm day—as in HD but for four 6-h periods during which a tropical cyclone is observed (or is estimated) to have attained tropical storm intensity winds
NTC	Net tropical cyclone activity—average seasonal percentage mean of named storms, named storm days, hurricanes, hurricane days, intense hurricanes, and intense hurricane days; gives overall indication of Atlantic basin seasonal hurricane activity
PDO	Pacific decadal oscillation
QBO	Quasi-biennial oscillation—a stratospheric (16–35-km altitude) oscillation of equatorial east–west winds that vary with a period of about 26–30 months or roughly 2 yr; typically blowing for 12–16 months from the east, then reversing and blowing 12–16 months from the west, then back to east again
SOI	Southern Oscillation index—a normalized measure of the surface pressure difference between Tahiti and Darwin, Australia
SST	Sea surface temperature
TC	Tropical cyclone—A large-scale circular flow occurring within the Tropics and subtropics that has its strongest winds at low levels, including hurricanes, tropical storms, and other weaker rotating vortices
TO	Tropical only—a term used to describe a tropical cyclone that develops without midlatitude influences
TOH	Tropical-only hurricanes
TONS	Tropical-only named storms
TS	Tropical storm—a tropical cyclone with maximum sustained winds between 39 (18 m s^{-1} or 34 kt) and 73 (32 m s^{-1} or 63 kt) mi h^{-1}

REFERENCES

Ballenzweig, E. M., 1959: Relation of long-period circulation anomalies to tropical storm formation and motion. *J. Meteor.*, **16,** 121–139.

Bjerknes, J., 1969: Atmospheric teleconnections from the tropical Pacific. *Mon. Wea. Rev.*, **97,** 103–172.

Blake, E. S., 2002: Prediction of August Atlantic basin hurricane activity. Dept. of Atmospheric Science Paper 719, Colorado State University, Fort Collins, CO, 80 pp.

Cook, K. H., 2001: A Southern Hemisphere wave response to ENSO with implications for southern Africa precipitation. *J. Atmos. Sci.*, **58,** 2146–2162.

DeMaria, M., 1996: The effect of vertical shear on tropical cyclone intensity change. *J. Atmos. Sci.*, **53,** 2076–2087.

Elsner, J. B., G. S. Lehmiller, and T. B. Kimberlain, 1996: Objective classification of Atlantic hurricanes. *J. Climate*, **9,** 2880–2889.

Gray, W. M., 1968: Global view of the origin of tropical disturbances and storms. *Mon. Wea. Rev.*, **96,** 669–698.

——, 1979: Hurricanes: Their formation, structure and likely role in the tropical circulation. *Meteorology over the Tropical Oceans*, D. B. Shaw, Ed., Royal Meteorological Society, 155–218.

——, 1984: Atlantic seasonal hurricane frequency. Part II: Forecasting its variability. *Mon. Wea. Rev.*, **112,** 1669–1683.

——, C. W. Landsea, and P. J. Klotzbach, 2002: Updated forecast of Atlantic seasonal hurricane activity and U.S. landfall strike probabilities for 2002. Dept. of Atmospheric Science Rep., Colorado State University, Fort Collins, CO, 26 pp.

Kalnay, E., and Coauthors, 1996: The NCEP/NCAR 40-Year Reanalysis Project. *Bull. Amer. Meteor. Soc.*, **77,** 437–471.

Klotzbach, P. J., 2002: Forecasting September Atlantic basin tropical cyclone activity at zero and one month lead times. Dept. of Atmospheric Science Paper 723, Colorado State University, Fort Collins, CO, 91 pp.

Knaff, J. A., 1998: Predicting summertime Caribbean pressure in early April. *Wea. Forecasting*, **13,** 740–752.

Krishnamurthy, V., and B. N. Goswami, 2000: Indian monsoon–ENSO relationship on interdecadal timescale. *J. Climate*, **13,** 579–595.

Landsea, C. W., 1993: A climatology of intense (or major) Atlantic hurricanes. *Mon. Wea. Rev.*, **121,** 1703–1713.

Larkin, N. K., and D. E. Harrison, 2001: Tropical Pacific ENSO cold events, 1946–95: SST, SLP, and surface wind composite anomalies. *J. Climate*, **14,** 3904–3931.

Maloney, E. D., and D. L. Hartmann, 2000: Modulation of hurricane activity in the Gulf of Mexico by the Madden–Julian oscillation. *Science*, **287,** 2002–2004.

Neter, J., W. Wasserman, and M. H. Kutner, 1983: *Applied Linear Regression Models.* Richard D. Irwin, 547 pp.

Neumann, C. J., M. B. Lawrence, and E. L. Caso, 1977: Monte Carlo significance testing as applied to statistical tropical cyclone prediction models. *J. Appl. Meteor.*, **16,** 1165–1174.

Pielke, R. A., Jr., and C. W. Landsea, 1998: Normalized hurricane damages in the United States: 1925–95. *Wea. Forecasting*, **13,** 621–631.

Rasmusson, E. M., and T. H. Carpenter, 1982: Variations in tropical sea surface temperatures and surface wind fields associated with the Southern Oscillation/El Niño. *Mon. Wea. Rev.*, **110,** 354–384.

Rodwell, M. J., D. P. Powell, and C. K. Folland, 1999: Oceanic forcing of the wintertime North Atlantic Oscillation and European climate. *Nature*, **398,** 320–323.

Shapiro, L. J., 1987: Month-to-month variability of the Atlantic tropical circulation and its relationship to tropical storm formation. *Mon. Wea. Rev.*, **115,** 2598–2614.

Simpson, R. H., 1974: The hurricane disaster potential scale. *Weatherwise*, **27,** 169, 186.

Thompson, D. W. J., and J. M. Wallace, 2000: Annular modes in the extratropical circulation. Part I: Month-to-month variability. *J. Climate*, **13,** 1000–1016.

Walker, G. T., 1923: Correlation in seasonal variations of weather VIII. *Mem. Ind. Meteor. Dept.*, **24,** 75–131.

——, 1924: World Weather IX. *Mem. Ind. Meteor. Dept.*, **24,** 275–332.

——, 1928: World Weather III. *Mem. Roy. Meteor. Soc.*, **17,** 97–106.

Wilks, D. S., 1995: *Statistical Methods in the Atmospheric Sciences: An Introduction.* Academic Press, 464 pp.

Wright, P. B., J. M. Wallace, T. P. Mitchell, and C. Deser, 1988: Correlation structure of the El Niño/Southern Oscillation phenomenon. *J. Climate*, **1,** 609–625.